ChemPubSoc Europe

DOI: 10.1002/chem.201402999

CHEMISTRY
A European Journal
Full Paper

Imaging Agents

Quantitative Fluorescence Ratio Imaging of Intralysosomal Chloride Ions with Single Excitation/Dual Maximum Emission

Ping Li, Shan Zhang, Nannan Fan, Haibin Xiao, Wen Zhang, Wei Zhang, Hui Wang, and Bo Tang*[a]

Abstract: Fluorescence ratio imaging is currently being used to quantitatively detect biologically active molecules in biosystems; however, two excitations of most existing fluorescent ratiometric probes account for cumbersome operating conditions for imaging. Thus, a fluorescent ratiometric probe, 6-methoxyquinolinium–dansyl (MQ-DS), for Cl^- with single excitation/dual maximum emission has been developed. MQ-DS can preferably localize into lysosomes and display excellent photostability. Upon excitation at a single wavelength, it responds precisely and instantaneously to changes in Cl^- concentrations, and it can be conveniently utilized to implement real-time fluorescence ratio imaging to quantitatively track alterations in Cl^- levels inside cells treated under various pH conditions, and also in zebrafish with acute wounds. The successful application of the new probe in bioimaging may greatly facilitate a complete understanding of the physiological functions of Cl^-.

Introduction

Chloride ions (Cl^-), which are the most abundant physiological anions, have a critical role in a great variety of cellular processes, including neurotransmission, regulation of cytoplasmic and vesicular pH, cellular volume, and charge balance.[1] As a result, Cl^- homeostasis alterations are associated with numerous diseases, such as lysosomal storage disease, cystic fibrosis, myotonia, and osteopetrosis.[2] Previous studies revealed that Cl^- was abundant in acidic subcellular regions, especially lysosomes. Lysosomes, which are membrane-bound cytoplasmic compartments, serve as a major degradative organelle in eukaryotic cells.[3] Their degradative functions for internalized macromolecules depend on maintaining an acidic environment. Indeed, there is a growing body of evidence that Cl^- permeability of lysosomes plays an important role in lysosomal acidification.[4] Therefore, monitoring lysosomal Cl^- has received increasing attention, especially by means of fluorescence imaging approaches combined with fluorescent probes due to high-resolution and sensitivity.[5]

Fluorescent ratiometric probes are considered to be extremely powerful bioimaging tools for biologically active molecules, because such ratios effectively suppress interference of intensity variations that result from probe concentration, optical path length, and excitation intensity.[6] Therefore, fluorescent ratio imaging is an effective approach for the quantitative detection of intracellular biologically active molecules. However, existing fluorescent ratiometric probes, including Cl^- probes, are mostly based on two-wavelength excitation.[7] Two excitations require more complicated instrumental settings, which obstruct the continuity of data collection in real time and cause difficulties in detection in diverse biological processes. The levels of intracellular biologically active molecules vary continuously with time. Thus, to accurately measure their concentrations, the development of fluorescent ratio imaging with a single excitation wavelength has attracted interest.[8] Nevertheless, due to electronic effects of the probe structure, it is difficult to pursue single excitation/dual maximum emission of the probe molecule, which still remains a big challenge. In view of the critical regulation role of chloride ions in physio- and pathological processes, precise imaging and quantification of Cl^- in live cells and tissues are highly desired and noteworthy.

To address this issue, we designed a series of new fluorescence ratiometric probes that consisted of two fluorophores with identical excitation wavelengths, that is, a Cl^--sensitive 6-methoxyquinolinium (MQ) group and a Cl^--insensitive dansyl (DS) group (Scheme 1). Importantly, emission peaks of the two fluorophores distinctly differ in wavelength when simultaneously excited at the same wavelength. Another reason for choosing DS is a dimethylamino group in its structure, which is comparable to commercial lysosome dyes and contributes to probe delivery into the lysosome through binding of H^+. To screen ideal ratio imaging probes, the two moieties are linked covalently through three different spacers, three methylenes (**1**), *N*-methylenepiperazine (**2**), and benzyl (MQ-DS), to modu-

[a] *Prof. P. Li, S. Zhang, N. Fan, Dr. H. Xiao, Dr. W. Zhang, W. Zhang, H. Wang, Prof. B. Tang*
College of Chemistry, Chemical Engineering and Materials Science
Collaborative Innovation Center of Functionalized Probes for Chemical Imaging, Key Laboratory of Molecular and Nano Probes
Ministry of Education, Shandong Normal University
Jinan 250014 (P.R. China)
E-mail: tangb@sdnu.edu.cn

Supporting information for this article is available on the WWW under http://dx.doi.org/10.1002/chem.201402999.

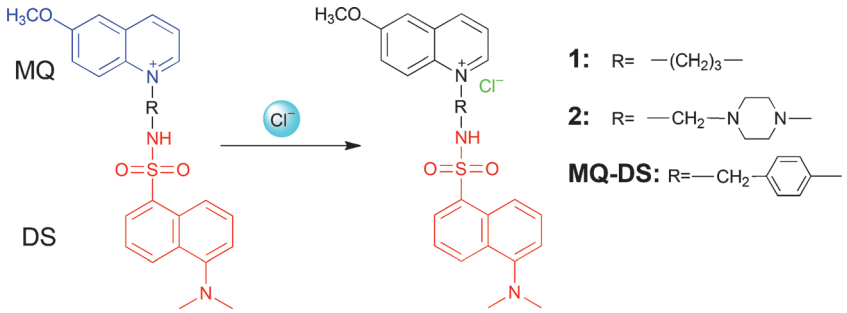

Scheme 1. Structures of the designed probes.

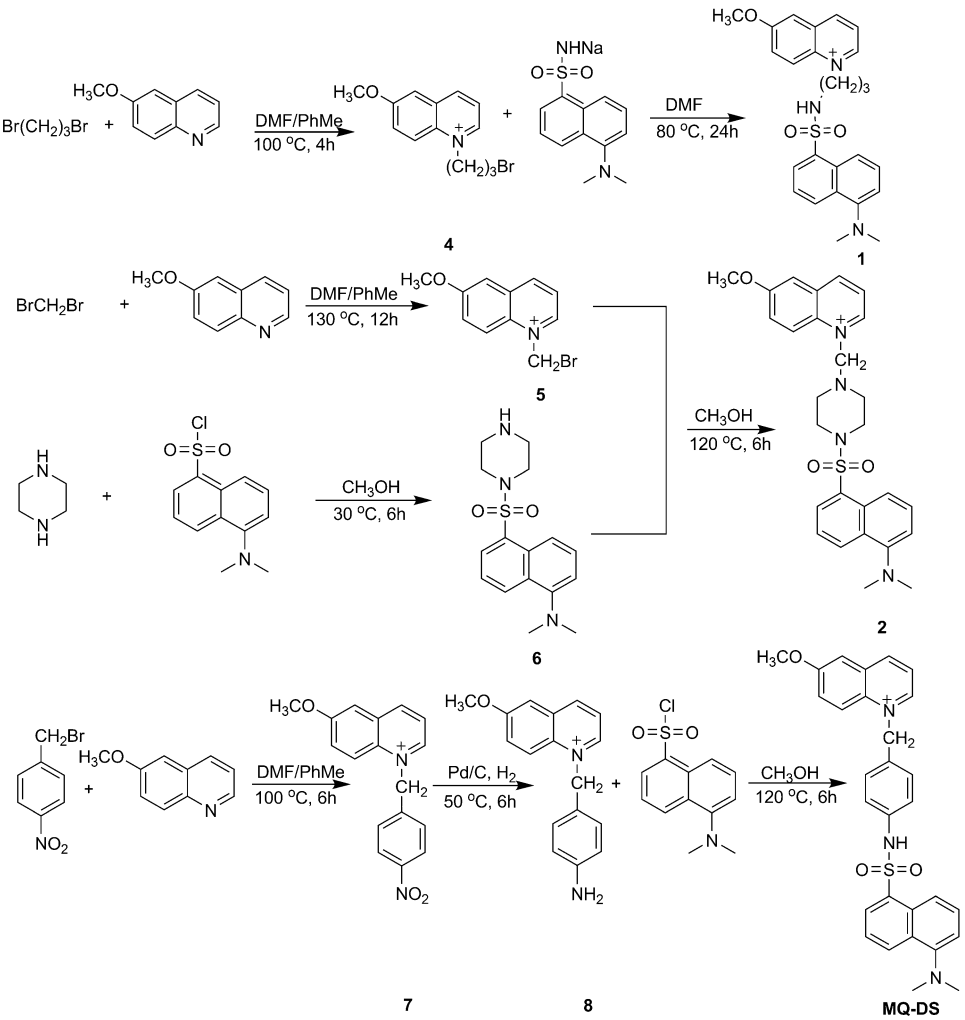

Scheme 2. Synthesis of compounds **1**, **2**, and MQ-DS.

late electronic effects.[9] Herein, we describe the synthesis and properties of these designed ratiometric probes.

Results and Discussion

The syntheses of compounds **1**, **2**, and MQ-DS are shown in Scheme 2. The spectroscopic properties of three compounds and their fluorescence responses to Cl^- were evaluated in detail.

Although all synthesized compounds show two well-separated emission bands upon excitation at a single wavelength, experimental results reveal that compounds **1** and **2** cannot reliably sense changes in Cl^- concentrations, whereas MQ-DS can, as shown in Figure S1 in the Supporting Information. Owing to no emission cross-talk between the two fluorophores, these two distinct measurable signals of maximum emission wavelengths ($\lambda = 440$ and 560 nm) are favorable to quantitative detection of Cl^- by using fluorescence ratio changes.

As expected, the presence of Cl^- brings about striking decline in the fluorescence intensity of MQ ($\lambda = 440$ nm) and, at the same time, the fluorescence intensity of the DS moiety ($\lambda = 560$ nm) remains essentially constant (Figure 1), which leads to enhancement of the fluorescence ratio between DS and MQ. The observed ratio (F_{560}/F_{440}) changes are proportional to Cl^- concentrations, and the linear regression equation was $F_{560}/F_{440} = 0.4801 + 0.0044[Cl^-]$ ($\times 10^{-3}$ M) with a correlation coefficient of 0.9937 (Figure S1c in the Supporting Information); the detection limit was calculated to be 0.18 mM. These results demonstrate that the linear response of MQ-DS to Cl^- concentrations within the physiological range (0–100 mM). In contrast to two excitations of existing fluorescent ratiometric probes, the single-wavelength excitation and well-separated dual maximum emission profiles can effectively overcome the cumbersome operation of imaging and the deviation of data collection, which greatly improve the accuracy and precision of Cl^- measurements.

To confirm whether MQ-DS could selectively detect Cl^-, we investigated interference from various biologically relevant anions (Figure S2 in the Supporting Information). When other anions were present, changes in the F_{560}/F_{440} ratio values were negligible. Once Cl^- was added to the above-mentioned

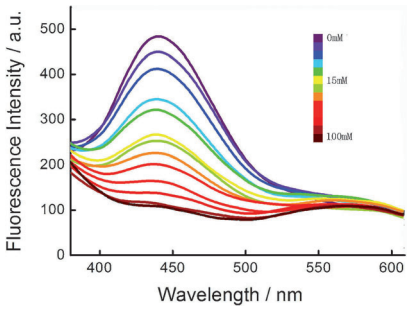

Figure 1. Fluorescence spectroscopic responses of 12 μM MQ-DS to Cl^- in 5.0 mM phosphate/citric acid buffer (pH 4.5). The Cl^- concentrations are from 0 to 100 mM. Fluorescence responses occur immediately upon mixing. The excitation wavelength was $\lambda = 330$ nm.

system, elevation of the ratio values appeared. Therefore, we can conclude that the ratiometric fluorescence response of MQ-DS is Cl^- selective. Furthermore, the effect of pH on the MQ-DS fluorescence ratio was studied. The fluorescence ratios of MQ-DS in the reaction system remained essentially constant from pH 4.5 to 7.5 (Figure 2). Thus, MQ-DS is believed to be pH

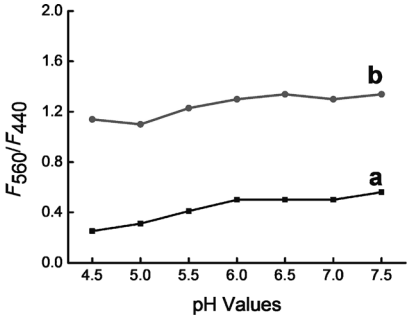

Figure 2. Effect of pH on the fluorescence ratio of MQ-DS (12 μM) in the absence (a) and presence (b) of Cl^- (100 mM).

insensitive. Additionally, some other aspects of MQ-DS were examined, and these experimental results indicated that MQ-DS was highly photostable (Figures S3 and S4 in the Supporting Information) with low cytotoxicity (Figure S5 in the Supporting Information).

A study of absorption spectra of MQ-DS shows that it exhibits its absorption bands centered at $\lambda = 330$ nm in phosphate/citric acid buffer (pH 4.5; Figure 3a) and cell extracts (Figure 3b), and apparently a wider band can be observed in cell extracts. In view of the clear absorption at $\lambda = 405$ nm in cell extracts, MQ-DS can be excited effectively by using a confocal fluorescence microscope equipped with a $\lambda = 405$ nm laser. We assessed the application of MQ-DS in bioimaging. First, we examined whether MQ-DS could preferably accumulate into lysosomes in costaining experiments with Lyso-Tracker DND-26 (a convenient commercially available intralysosomal dye). From analysis of merged images (Figure 4C and F) captured in human hepatoma cells (HepG2) loaded simultaneously with MQ-DS (MQ: blue channel; Figure 4A, and DS: red channel;

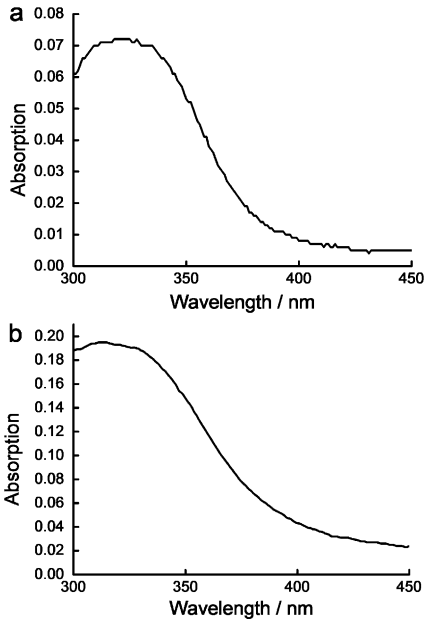

Figure 3. Absorption spectra of MQ-DS (48 μM) in 5.0 mM phosphate/citric acid buffer (pH 4.5) (a) and cell extracts (b).

Figure 4E) and Lyso-Tracker DND-26 (green channel; Figure 4B), we found that distribution domains of the two compounds overlapped well, which indicated that their localization patterns were similar. The colocalization coefficient was further calculated to be 0.95. These results suggest that MQ-DS is readily taken up by cells and targeted to lysosomes. This evidence substantiates the postulation that MQ-DS is a robust ratiometric sensor to visualize changes in Cl^- within lysosomes.

Next we studied Cl^- fluctuations in HepG2 cells incubated with Tyrode's solution (containing 136.9 mM potassium) containing various concentrations of Cl^-. Fluorescence ratio imaging is readily carried out with optical windows for MQ (from $\lambda = 410$ to 505 nm, blue; Figure 5a) and DS (from $\lambda = 525$ to 620 nm, red; Figure 5b) at a single excitation wavelength of 405 nm. The ratio of fluorescence intensity between the red and blue channels for MQ-DS-stained cells directly reflect Cl^- levels in HepG2 incubated with Tyrode's solution (Figure 5c), according to the fluorescence intensity ratio scale and graph of output data. Moreover, there was good linearity between the fluorescence intensity ratio and Cl^- concentrations in the range of 0–140 mM, as depicted in Figure 5. The linear regression equation was $F_{red}/F_{blue} = 0.3073 + 0.0047[Cl^-]$ ($\times 10^{-3}$ M) with a correlation coefficient of 0.9946 (Figure 5I). Similar experiments in cell extracts gave identical results (Figure S6 in the Supporting Information). These results unequivocally prove that MQ-DS is a reliable ratiometric sensor that can conveniently image changes in intracellular Cl^- by single wavelength excitation.

It is widely accepted that chloride ion channels in the cell membrane play essential roles in maintaining cellular osmolality and intracellular pH stability. As a result, pH changes may alter intracellular chloride levels because Cl^- is the main counterion used to balance H^+ accumulation.[10] We studied wheth-

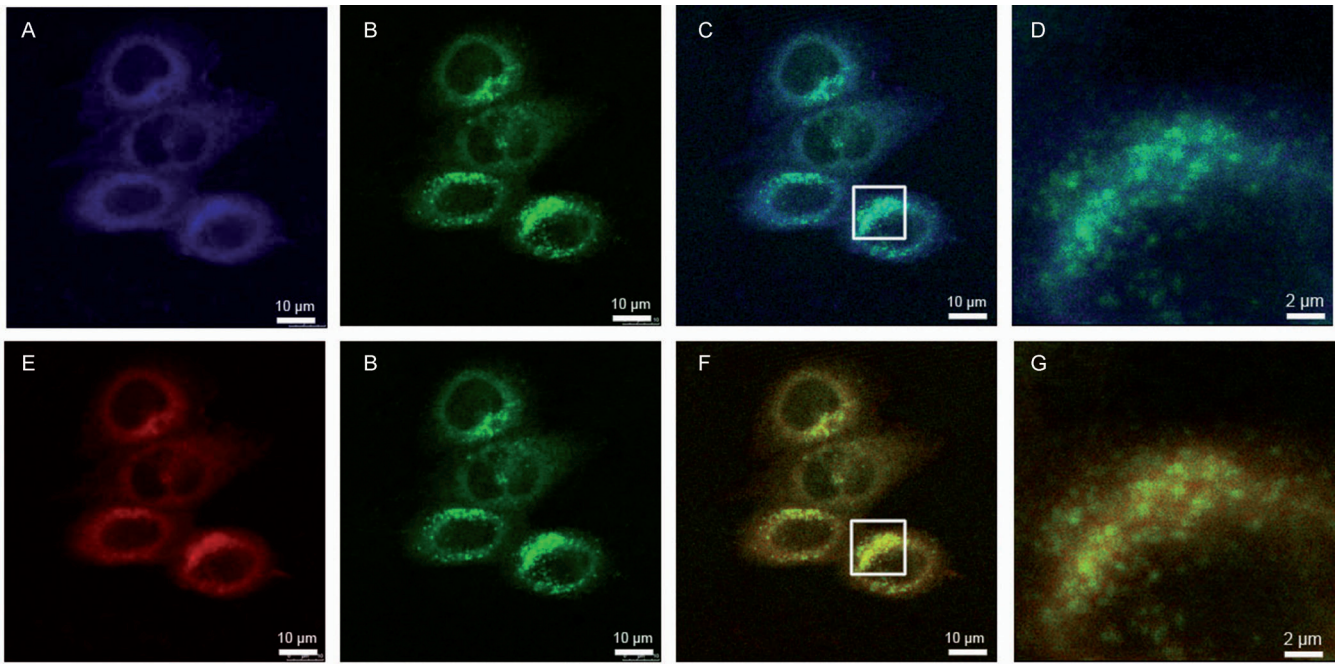

Figure 4. Confocal fluorescence images of live HepG2 cells costained with 100 μM MQ-DS and 5.0 μM Lyso-Tracker DND-26 for 15 min at 37 °C. A) Fluorescence image of the MQ moiety (blue). B) Fluorescence images of Lyso-Tracker DND-26 (green). C) Merged image from A) and B). D) Higher magnification of the area in a box in C). E) Fluorescence image of the DS moiety (red). F) Merged image from E) and B). G) Higher magnification of the area in a box in F). Upon excitation at $\lambda = 405$ nm, the blue and red channels were collected at $\lambda = 410–505$ and 525–620 nm, respectively; the green channel was collected at $\lambda = 505–520$ nm provided with excitation of $\lambda = 488$ nm wavelength.

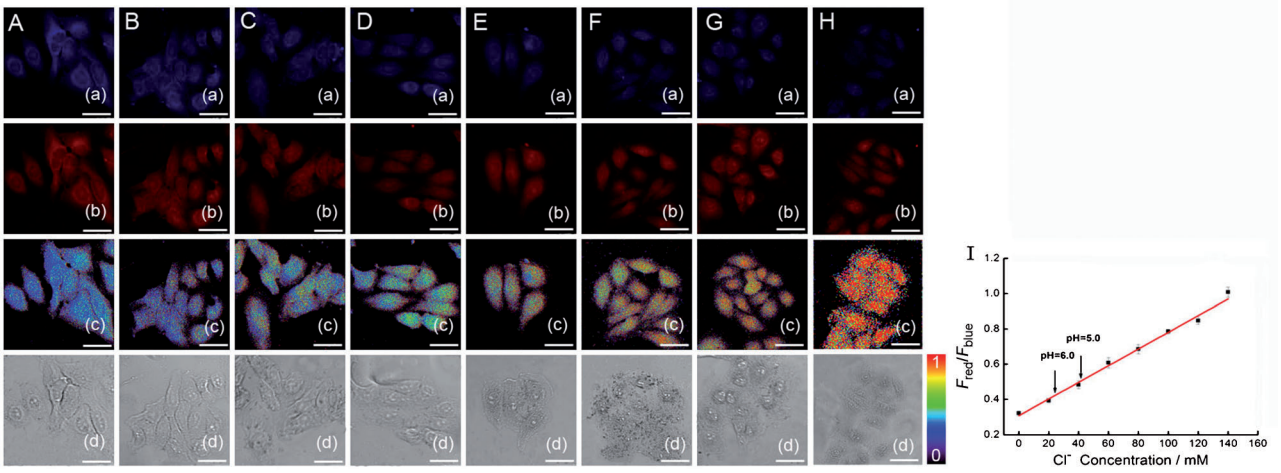

Figure 5. Responses of MQ-DS (100 μM) to Cl^- in HepG2 cells. Columns A to H represent Cl^- concentrations of 0, 20, 40, 60, 80, 100, 120, and 140 mM, respectively, in the media. a) Fluorescence images of MQ (blue channel) and b) DS (red channel). c) Ratio images generated directly from the red and blue channels (F_{red}/F_{blue}). d) Bright-field images of cells. Scale bars are 25 μm. I) Intracellular Cl^- calibration curve of MQ-DS in HepG2 cells from A(c)–H(c).

er the probe could visualize changes of Cl^- concentrations in liver cancer cells (HepG2) incubated under various pH conditions. Imaging experiments were performed at pH 5.0 and 6.0, respectively (Figure 6), and displayed apparent differences in fluorescence ratio inside the cells. By measuring the fluorescent intensity of cells imaged at different pH values, the corresponding Cl^- concentrations were calculated to be (39.76 ± 1.54) (pH 5.0) and (23.48 ± 0.87) mM (pH 6.0) respectively (Figure 5I). According to the linear regression equation obtained in liver cancer cells, Cl^- concentrations were calculated based on average values of fluorescence ratio in four areas (white circles in Figure 6c). These results strongly suggest that the probe is able to quantify Cl^- fluctuations in live cells through fluorescent ratio imaging.

It is reported that intracellular Cl^- concentrations will increase when myocardial ischemia happens, and a low extracellular Cl^- concentration can significantly a delay in the ischemia-induced increase in Cl^- concentration.[11] MQ-DS was used

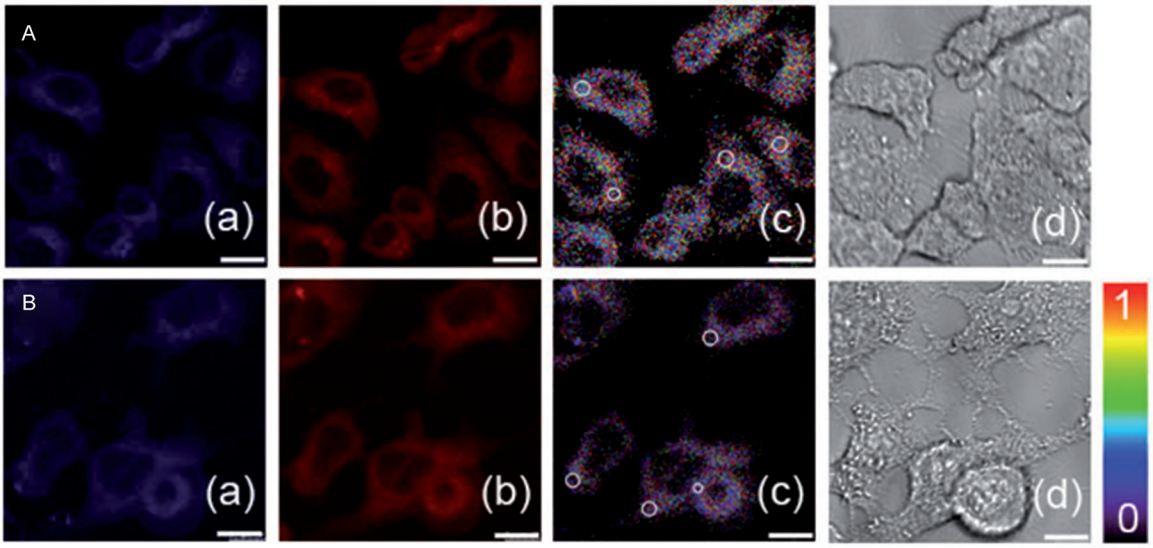

Figure 6. Pseudocolor fluorescence ratio images (F_{red}/F_{blue}) of HepG2 cells labelled with MQ-DS (100 μM) at pH 5.0 (A) and 6.0 (B). a) The blue channel was collected at $\lambda = 410–505$ nm. b) The red channel was collected at $\lambda = 525–620$ nm with excitation at $\lambda = 405$ nm. c) Ratio images generated directly from the red and blue channels. d) Bright-field images of cells. Scale bars are 10 μm.

to visualize fluctuations of Cl^- levels during myocardial ischemia, and the fluorescence ratio images are displayed in Figure 7. Upon the treatment of ischemia in ventricular myocytes, there was a gradual elevation in Cl^- levels from 0 ((9.46 ± 0.43) mM) to 75 min ((77.95 ± 0.61) mM; Figure 7G). These dynamic imaging results clearly demonstrate that MQ-DS can serve for real-time quantitative tracking of the changes in Cl^- concentrations within live cells.

We further applied MQ-DS for detecting Cl^- fluctuations in vivo. In a previous investigation, it was found that acute wounds were closely associated with high H^+ levels.[12] Meanwhile, Cl^- is the main counterion used to balance H^+ accumulation, and accordingly, an increase in H^+ might cause a rapid rise in Cl^- within living systems.[10] Herein, we tested whether MQ-DS could visualize real-time changes in Cl^- within injured zebrafish because H^+ increase induced by injury should accompany an increase in Cl^- levels. In zebrafish loaded with MQ-DS, 10 min after trauma, we observed an increase in the fluorescence intensity ratio between the red and blue channels (Figure 8). A larger ratio means that more Cl^- is present ((43.84 ± 1.23) mM, 10 min), compared with 0 min ((19.01 ± 0.61) mM), which confirms that Cl^- influx acts to control pH; this is consistent with previous reports. These results further demonstrate the value of this fluorescence ratiometric probe for quantitative and dynamic tracking of Cl^- in vivo.

Conclusion

We presented the synthesis, properties, and biological application of MQ-DS, a new fluorescence ratio imaging probe for Cl^- in lysosomes, which allowed for single excitation/dual maximum emission ratio detection of intralysosomal Cl^- for the first time. The single-wavelength excitation and well-separated dual maximum emission wavelengths are beneficial for precise and accurate monitoring of real-time changes in Cl^- levels. MQ-DS also displays excellent selectivity for Cl^-, less cytotoxicity, and good membrane permeability. Furthermore, we used MQ-DS to accurately quantify intracellular Cl^- concentrations under various pH conditions or myocardial ischemia. In particular, MQ-DS dynamically visualized real-time quantitative fluctuations of Cl^- in zebrafish after acute injury. Altogether, these results established that the new fluorescence ratiometric probe was a potent tool to reliably and quantitatively visualize Cl^- in live cells and tissues; these results can contribute to completely unravel the biological functions of Cl^-. Furthermore, this single excitation/dual maximum emission result provides a new strategy for precise and accurate detection of other biological molecules in live cells and in vivo.

Experimental Section

Materials and reagents

Solutions of compounds **1**, **2**, and MQ-DS (DMSO, 0.1 mM) could be maintained in a refrigerator at 4 °C. Unless stated otherwise, solvents were dried by distillation. All chemicals were available commercially and the solvents were purified by conventional methods before use. MQ (≥98%) and 3-(4,5-dimethylthiazol-2-yl)-2,5-diphenyltetrazolium bromide (MTT) were purchased from Sigma Aldrich. 1,3-Dibromopropane (≥98%), 5-(dimethylamino)-1-naphthalenesulfonamide (≥99%), 5-dimethylamino-1-naphthalenesulfonyl chloride (≥98%), dibromomethane (≥99%), piperazine (≥99%), and 4-nitrobenzyl bromide (≥99%) were all purchased from Aladdin Chemical Company (Shanghai, P.R. China). Lyso-Tracker DND-26 was from a molecular probes company. All other reagents and solvents were purchased from commercial sources and of analytical reagent grade, unless indicated otherwise. HepG2 (Human hepatocellular liver carcinoma cell line) and H9c2 (2-1) cells (Adult rat ventricular myocytes) were purchased from the Committee on Type Culture Collection of Chinese Academy of Sciences (Shanghai, P.R. China). Sartorius ultrapure water (18.2 MΩ cm) was used throughout. Universal buffer medium (0.1 M citric acid, 0.1 M K_2PO_4, 0.1 M

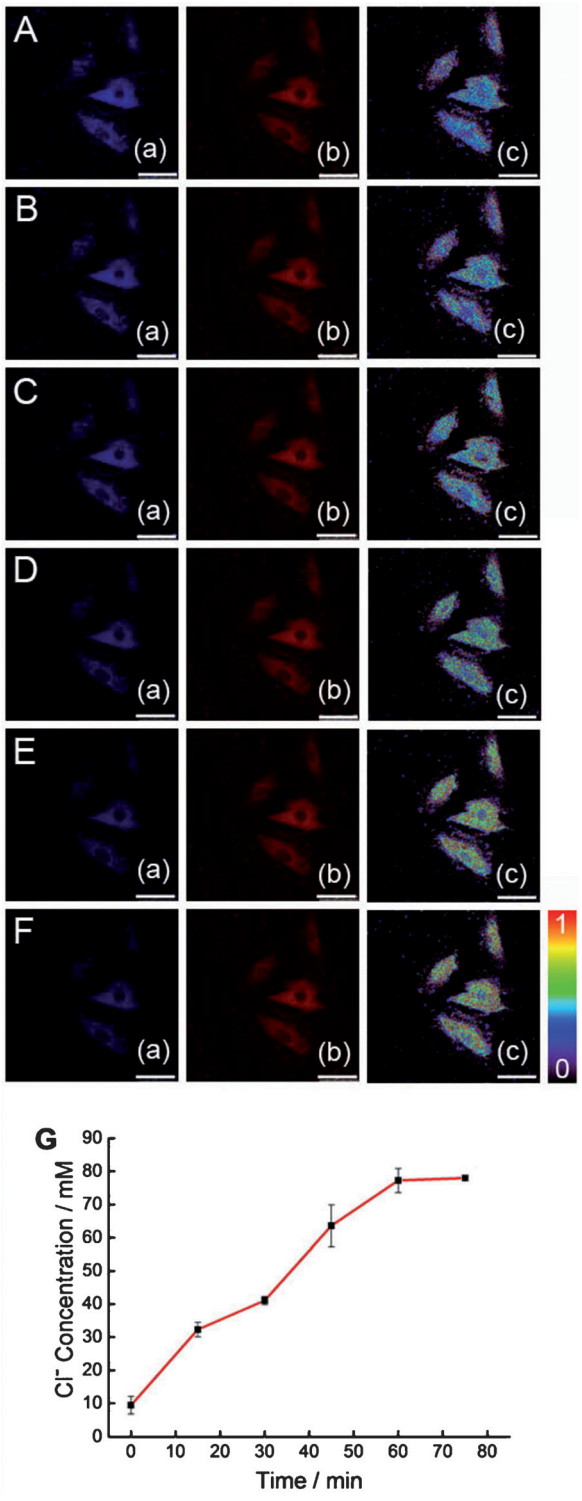

Figure 7. Pseudocolor ratiometric imaging of live ventricular myocytes labelled with MQ-DS (100 μM). Rows A to F represent simulated ischemia groups at 0, 15, 30, 45, 60, and 75 min, respectively. Fluorescence images of a) MQ (blue channel) and b) DS (red channel). c) Ratio images generated directly from the red and blue channels (F_{red}/F_{blue}). d) Bright-field images of cells. Scale bars are 50 μm. G) Variation of Cl^- concentration with time; this was calculated from output data of A(c)–F(c).

$Na_2B_4O_7$, 0.1 M Tris, 0.1 M KCl) was adjusted to the corresponding pH by using solutions of 98.3% sulfuric acid and saturated NaOH.

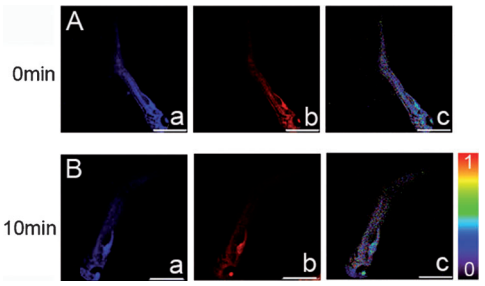

Figure 8. Ratiometric images of live zebrafish upon trauma: A) 0 and B) 10 min. Zebrafish cut near the tail were pretreated with 200 μM MQ-DS in water for 15 min. Fluorescence images of a) MQ (blue channel) and b) DS (red channel). c) Ratio images generated directly from the red and blue channels. Scale bars are 1 mm.

Instrumentation

NMR spectra were recorded mainly on a Bruker Avance II-400 Fourier transform spectrometer operating at 600 MHz for ^1H and at 150 MHz for ^{13}C. The mass spectra were obtained on a Bruker maXis ultra-high resolution-TOF MS system and an Agilent 1200LC-6520 Q-TOF LC/MS (US80620227) instrument. Fluorescence spectra measurements were performed by using a Cary Eclipse fluorescence spectrophotometer. The slit width was 20 nm for both excitation and emission. Samples were contained in 2.0 mm path length quartz cuvettes. In experiments with cell extracts, the slit width was 5 nm for both excitation and emission, and samples were contained in 1.0 mm path length quartz cuvettes. Cell extracts were prepared by using a BILON92-IIL ultrasonic disintegrator (Shanghai Bilon Materials Inc.).

Cell culture

HepG2 cells and H9c2 (2-1) cells were cultured in Dulbecco's modified eagle medium (DMEM) containing 10% fetal bovine serum (FBS), 1% penicillin, and 1% streptomycin at 37 °C (w/v) in a 5% CO_2/95% air incubator MCO-15AC (Sanyo, Tokyo, Japan). The concentrations of counted cells were adjusted to 1×10^6 cells mL^{-1} for confocal imaging in high-glucose DMEM (4.5 g of glucose/L) supplemented with 10% FBS, $NaHCO_3$ (2 ng L^{-1}), and 1% antibiotics (penicillin/streptomycin, 100 U/mL). Cultures were maintained at 37 °C under a humidified atmosphere containing 5% CO_2.

Cell extracts

Cell concentration was adjusted to 1×10^6 cells mL^{-1}. HepG2 cells were incubated with Tyrode's solution containing Cl^- (Cl^--treated group) and without Cl^- (blank group) for 3 h at 37 °C in an incubator. The cells were suspended in a volume of phosphate/citric acid buffer (pH 4.5) and disrupted for 6 min in an ultrasonic disintegrator (<4 °C). The broken cell suspension was centrifuged at 12000 rpm for 30 min and the pellet was discarded to give the cell extracts.

Fluorescence imaging

Fluorescent images were acquired on a Leica TCS SP5 confocal laser scanning microscope with an objective lens (40× and 20×). The excitation wavelengths were $\lambda=405$ and 488 nm respectively. Cell imaging was carried out after washing cells with phosphate/citric acid buffer three times. Fluorescence images of MQ-DS were obtained at an excitation wavelength of $\lambda=405$ nm. Blue and red channels were collected at $\lambda=410$–505 and 525–620 nm, respec-

tively, and ratio images were generated directly from the red and blue channels.

For experiments of cellular localization, ventricular myocytes were costained with 100 μM MQ-DS and 5.0 μM Lyso-Tracker DND-26 for 15 min at 37 °C. For confocal fluorescence images, MQ-DS was excited at $\lambda = 405$ nm and Lyso-Tracker DND-26 was excited at $\lambda = 488$ nm; both were collected at $\lambda = 505$–520 nm.

For experiments of linearity between the fluorescence intensity ratio and Cl^- concentrations, HepG2 cells were treated with Tyrode's solution[13] (containing 136.9 mM potassium) containing various concentrations of Cl^-, nigericin (5 μM), and tributyltin (10 μM) for 30 min at 37 °C, and then incubated with MQ-DS (100 μM) for 15 min.

For cell images under various pH conditions, HepG2 cells were incubated with universal buffer (pH 5.0 and 6.0; $C_{Cl^-} = 100$ mM) for 1 h at 37 °C, then incubated with MQ-DS (100 μM) for 15 min.

For experiments of myocardial ischemia, ventricular myocytes were incubated with MQ-DS (100 μM) for 15 min at 37 °C, washed twice with ischemic solution (sodium lactate instead of glucose from Tyrode's solution), then imaged by using a confocal laser scanning microscope every 15 min after adding the ischemic solution.

Zebrafish were incubated with 200 μM MQ-DS for 15 min, then washed three times with water. The zebrafish were anesthetized with 5% diethyl ether. After cutting of the tail (0 and 10 min), the zebrafish were imaged by using a confocal laser scanning microscope. The zebrafish were obtained from Biology Institute of Shangdong Academy of Sciences. The experiments were approved by the institutional committee. All the animal experiments were carried out in accordance with the relevant laws and guidelines issued by the Ethical Committee of Shangdong Academy of Sciences.

MTT assay

Ventricular myocytes (10^6 cell mL^{-1}) were dispersed within replicate 96-well microtiter plates to a total volume of 200 μL per well. Plates were maintained at 37 °C in a 5% CO_2/95% air incubator for 24 h. Then ventricular myocytes were incubated for 16 h with different probe concentrations of 1.0×10^{-6}, 1.0×10^{-5}, 1.0×10^{-4}, and 1.0×10^{-3} M. MTT solution (5 mg mL^{-1}, phosphate-buffered saline (PBS)) was then added to each well. After 4 h, the remaining MTT solution was removed, and DMSO (150 μL) was added to each well to dissolve the formazan crystals. Absorbance was measured at $\lambda = 490$ nm in a Triturus microplate reader. Calculation of IC50 values was performed according to the Huber and Koella method.[14]

Synthesis

Compound 4: 1,3-Dibromopropane (2.1708 g, 10.8 mmol) and 6-methoxyquinoline (0.8586 g, 5.4 mmol) were dissolved in DMF/PhMe (3:2, 10 mL) and heated at 100 °C for 4 h. After cooling to room temperature, the mixture was filtered. The solid was washed several times with acetone. Compound **4** was collected by centrifugation as an orange solid (≈75%). HRMS *m/z* calcd for $C_{13}H_{15}BrNO$: 280.0331 $[M+H]^+$; found: 280.0328.

Compound 1: Dansylamide sodium salt (0.1360 g, 0.5 mmol) and **4** (0.2800 g, 1.0 mmol) were dissolved in DMF (8 mL), and heated at 80 °C for 24 h. An orange solution was obtained, which was purified by column chromatography on silica gel by eluting with hexane/ethyl acetate/methanol (1/2/0.5, v/v/v) to give **1** (≈50%). ^{1}H NMR (600 MHz, $CDCl_3$): $\delta = 1.99$–2.02 (d, 2H), 2.21–2.23 (m, 2H), 2.87–2.89 (m, 6H), 3.87 (t, 3H), 4.29–4.36 (m, 2H), 4.79 (s, 1H), 7.08 (s, 1H), 7.16–7.19 (d, 1H), 7.38–7.40 (m, 2H), 7.41–7.44 (t, 1H), 7.56–7.58 (t, 1H), 8.00–8.02 (d, 1H), 8.06–8.07 (d, 1H), 8.14–8.16 (d, 1H), 8.31–8.32 (d, 1H), 8.48–8.50 (d, 1H), 8.77 ppm (d, 1H); ^{13}C NMR (150 MHz, DMSO): $\delta = 151.7$, 129.7, 129.4, 128.9, 128.1, 123.9, 119.9, 119.4, 115.5, 73.7, 57.6, 56.5, 45.5, 40.8, 40.5, 19.0 ppm; HRMS: *m/z*: calcd for $C_{25}H_{28}N_3O_3S$: 450.1846 $[M+H]^+$; found: 450.1906.

Compound 5: 1,2-Dibromomethane (1.8684 g, 10.8 mmol) and 6-methoxyquinoline (0.8586 g, 5.4 mmol) were mixed in DMF/PhMe (3:2, 10 mL), and heated at 130 °C for 12 h. After cooling to room temperature, the mixture was filtered. The solid was washed several times with acetone. Compound 5 was obtained by centrifugation as a white solid (≈65%).

Compound 6: Piperazine (0.5618 g, 6.5 mmol) and dansyl chloride (0.1980 g, 5.4 mmol) were added to anhydrous methanol (10 mL), and pyridine (0.5 mL) was used as a catalyst. The mixture was stirred at 30 °C for 6 h under argon. The solution was purified by column chromatography on silica gel, eluting with hexane/ethyl acetate (3/1, v/v), to give **6** (≈60%). HRMS: *m/z* calcd for $C_{16}H_{21}N_3O_2S$: 320.1427 $[M+H]^+$; found: 320.1331.

Compound 2: Compound **6** (1.7280, 5.4 mmol) was dissolved in anhydrous methanol (5 mL) and triethylamine (0.5 mL) was added as a catalyst. The mixture was heated to 120 °C and **5** (1.3500 g, 5.4 mmol) was added dropwise to the solution. After 6 h, a yellow liquid was obtained. The crude product was purified by column chromatography on silica gel, eluting with hexane/ethyl acetate/methanol (1/3/0.2, v/v/v), to obtain probe **2** (≈47%). ^{1}H NMR (600 MHz, $CDCl_3$): $\delta = 2.02$–2.06 (m, 4H), 2.89–2.92 (m, 6H), 4.10 (s, 2H), 7.08 (s, 1H), 7.21–7.23 (t, 1H), 7.33–7.36 (m, 2H), 7.54–7.56 (t, 2H), 7.93–7.96 (d, 1H), 8.12–8.13 (d, 1H), 8.19–8.20 (d, 1H), 8.40–8.41 (d, 1H), 8.60–8.61 (d, 1H), 8.73 ppm (d, 1H); ^{13}C NMR (150 MHz, DMSO): $\delta = 159.3$, 144.0, 143.0, 136.2, 130.6, 128.9, 126.6, 124.6, 123.4, 123.0, 122.7, 107.0, 56.53, 49.0, 40.8, 40.6, 31.1 ppm; HRMS: *m/z* calcd for $C_{27}H_{31}N_4O_3S$: 491.2111 $[M+H]^+$; found: 491.2754.

Compounds 7 and 8: 4-Nitrobenzyl bromide (2.3331 g, 10.8 mmol) was added to 6-methoxyquinoline (1.7172 g, 10.8 mmol) in DMF/PhMe (3/2, 10 mL). The reaction temperature was kept at 100 °C for 6 h. The orange solution was obtained and filtered. Solid **7** (yield: ≈75%) was washed several times with acetone. The product was dissolved in methanol and then Pd/C was added before H_2 was introduced into the mixture. The solution was stirred at 50 °C for 6 h and the solvent was removed on a rotary evaporator. Compound **8** was obtained as a red solid (≈60%). HRMS: *m/z* calcd for $C_{17}H_{17}N_2O$: 265.1335 $[M+H]^+$; found: 265.1137.

MQ-DS: Compound **8** (0.1315 g, 0.5 mmol) and dansyl chloride (0.135 g, 0.5 mmol) were dissolved in anhydrous methanol (5 mL) and pyridine (0.5 mL) was added as the catalyst. The mixture was stirred at 120 °C for 6 h under argon, and purified by column chromatography on silica gel, eluting with hexane/ethyl acetate (3:1, v/v), to give MQ-DS (≈60%). ^{1}H NMR (600 MHz, $CDCl_3$): $\delta = 2.87$–2.89 (m, 6H), 3.87 (t, 3H), 4.29 (s, 2H), 4.82 (s, 1H), 6.92–6.93 (d, 2H),7.08–7.09 (d, 3H), 7.16–7.18 (d, 1H), 7.35–7.40 (m, 2H), 7.41–7.43 (t, 1H), 7.53–7.56 (t, 1H), 8.00–8.02 (d, 1H), 8.06–8.07 (d, 1H), 8.16–8.17 (d, 1H), 8.34–8.35 (d, 1H), 8.48–8.49 (d, 1H), 8.77 ppm (d, 1H); ^{13}C NMR (150 MHz, $CDCl_3$): $\delta = 157.7$, 152.1, 147.9, 144.3, 135.9, 135.0, 134.9, 134.2, 130.8, 130.3, 129.8, 129.6, 129.3, 128.6, 128.5, 123.1, 122.3, 121.4, 121.3, 118.5, 115.2, 105.1, 77.0, 76.8, 74.0, 58.0, 55.5, 45.4, 29.7 ppm; MS: *m/z*: 160.1, 371.1.

Acknowledgements

This work was supported by the 973 Program (2013CB933800), National Natural Science Foundation of China (21227005, 21390411, 91313302, 21035003, and 21205073) and Program for Chang jiang Scholars and Innovative Research Team in University.

Keywords: anions · chlorine · fluorescence · imaging agents · lysosomes

[1] a) E. K. Hoffmann, P. B. Dunham, *Int. Rev. Cytol.* **1995**, *161*, 173 – 262; b) P. Bregestovski, T. Waseem, M. Mukhtarov, *Front. Mol. Neurosci.* **2009**, *2*, 108 – 120.

[2] a) R. Planells-Cases, T. J. Jentsch, *Biochim. Biophys. Acta* **2009**, *1792*, 173 – 189; b) M. C. Koch, K. Steinmeyer, C. Lorenz, K. Ricker, F. Wolf, M. Otto, B. Zoll, F. Lehmann-Horn, K. H. Grzeschik, T. J. Jentsch, *Science* **1992**, *257*, 797 – 800.

[3] a) S. Kornfeld, I. Mellman, *Annu. Rev. Cell Biol.* **1989**, *5*, 483 – 525; b) W. Hunziker, H. J. Geuze, *Bioessays* **1996**, *18*, 379 – 389.

[4] a) A. R. Graves, P. K. Curran, C. L. Smith, J. A. Mindell, *Nature* **2008**, *453*, 788 – 792; b) S. Weinert, S. Jabs, C. Supanchart, M. Schweizer, N. Gimber, M. Richter, J. Rademann, T. Stauber, U. Kornak, T. J. Jentsch, *Science* **2010**, *328*, 1401 – 1403.

[5] a) T. Nagai, K. Ibata, E. S. Park, M. Kubota, K. Mikoshiba, A. Miyawaki, *Nat. Biotechnol.* **2002**, *20*, 87 – 90; b) A. S. Verkman, *Am. J. Physiol.* **1990**, *259*, C375 – C388; c) N. Marandi, A. Konnerth, O. Garaschuk, *Pflügers Archiv.* **2002**, *445*, 357 – 365; d) P. Li, W. Zhang, K. Li, X. Liu, H. Xiao, W. Zhang, B. Tang, *Anal. Chem.* **2013**, *85*, 9877 – 9881.

[6] a) S. R. Adams, A. T. Harootunian, Y. J. Buechler, S. S. Taylor, R. Y. Tsien, *Nature* **1991**, *349*, 694 – 697; b) D. W. Domaille, L. Zeng, C. J. Chang, *J. Am. Chem. Soc.* **2010**, *132*, 1194 – 1195; c) X. Wang, J. Sun, W. Zhang, X. Ma, J. Lv, B. Tang, *Chem. Sci.* **2013**, *4*, 2551 – 2556; d) R. G. Painter, G. Wang, *Anal. Chem.* **2006**, *78*, 3133 – 3137; e) P. Li, T. Xie, N. Fan, K. Li, B. Tang, *Chem. Commun.* **2012**, *48*, 2077 – 2079; f) N. D. Sonawane, F. C. Szoka, Jr., A. S. Verkman, *J. Biol. Chem.* **2003**, *278*, 44826 – 44831; g) L. Albertazzi, M. Brondi, G. M. Pavan, S. S. Sato, G. Signore, B. Storti, G. M. Ratto, F. Beltram, *Plos One* **2011**, *6*, e28450; h) O. Markova, M. Mukhtarov, E. Real, Y. Jacob, P. Bregestovski, *J. Neurosci. Methods* **2008**, *170*, 67 – 76.

[7] a) X. Peng, Z. Yang, J. Wang, J. Fan, Y. He, F. Song, B. Wang, S. Sun, J. Qu, J. Qi, M. Yan, *J. Am. Chem. Soc.* **2011**, *133*, 6626 – 6635; b) M. Taki, M. Desaki, A. Ojida, S. Iyoshi, T. Hirayama, I. Hamachi, Y. Yamamoto, *J. Am. Chem. Soc.* **2008**, *130*, 12564 – 12565.

[8] a) S. Bassnett, L. Reinisch, D. C. Beebe, *Am. J. Physiol.* **1990**, *258*, C171 – C178; b) C. J. Chang, J. Jaworski, E. M. Nolan, M. Sheng, S. J. Lippard, *Proc. Natl. Acad. Sci. USA* **2004**, *101*, 1129 – 1134; c) E. M. Nolan, S. J. Lippard, *J. Am. Chem. Soc.* **2007**, *129*, 5910 – 5918.

[9] S. Jayaraman, J. Biwersi, A. S. Verkman, *Am. J. Physiol. Cell Physiol.* **1999**, *276*, C747 – C757.

[10] D. Arosio, F. Ricci, L. Marchetti, R. Gualdani, L. Albertazzi, F. Beltram, *Nat. Methods* **2010**, *7*, 516 – 518.

[11] Z. F. Lai, K. Nishi, *Am. J. Physiol. Heart Circ. Physiol.* **1998**, *275*, H1613 – H1619.

[12] J. Llopis, J. M. McCaffery, A. Miyawaki, M. Farquhar, R. Y. Tsien, *Proc. Natl. Acad. Sci. USA* **1998**, *95*, 6803 – 6808.

[13] J. Liu, Z. F. Lai, X. D. Wang, N. Tokutomi, K. Nishi, *J. Cardiovasc. Pharmacol.* **1998**, *31*, 558 – 567.

[14] W. Huber, J. C. Koella, *Acta Trop.* **1993**, *55*, 257 – 261.

Received: April 8, 2014
Published online on August 5, 2014